
The α - and β -Relaxation Processes of Polymeric Chitosan from Squid Gladii as Revealed by Dynamic Mechanical Analysis

Juma Hanif, John Onyango Agumba*, Katana Gona Gabriel

Physics Department, Pwani University, Kilifi, Kenya

Email address:

j.agumba@pu.ac.ke (J. O. Agumba)

*Corresponding author

To cite this article:

Juma Hanif, John Onyango Agumba, Katana Gona Gabriel. The α - and β -Relaxation Processes of Polymeric Chitosan from Squid Gladii as Revealed by Dynamic Mechanical Analysis. *American Journal of Mechanical and Materials Engineering*. Vol. 2, No. 4, 2018, pp. 40-45.

doi: 10.11648/j.ajmme.20180204.12

Received: November 21, 2018; **Accepted:** December 13, 2018; **Published:** January 22, 2019

Abstract: Dynamic mechanical analysis, DMA, is a technique that can be used to study the mechanical properties of polymeric biomaterials so as to help unveil the physiological environments in which they can be applied. In this study, mechanical properties of chitosan (poly (β -(1 \rightarrow 4)-N-acetyl-D-glucosamine)) thin films extracted from squid gladii found along the coastal areas of Kilifi and Mombasa in Kenya have been systematically investigated using DMA technique. From the study, chitosan thin film have shown a β - relaxation process occurring between 293K and 323K and the α - relaxation process hereby referred to as glass transition (T_g) occurring between 393K and 423K. Additionally, the chitosan films under the study are viscoelastic with very low mechanical damping suggesting that they have very high rigidity and resistance to deformation. The results from this study have thus given us an insight of the operating temperature range of the biomaterial.

Keywords: α - Relaxation, β -Relaxation, Squid Gladii, Chitin, Chitosan, Acetylation, Deacetylation

1. Introduction

Progress in soft condensed matter surfaces at the molecular level is today forming the building blocks for the creation of the next generation materials and devices in practically all scientific areas. The unique structure of polymers can yield desirable macro-physical attributes related to their mechanics, chemistry and thermo stability. Thin films have mechanical, electrical, magnetic and optical properties which differ from those of the bulk materials. Currently, the need for thin film materials and devices are creating new opportunities for the development of new processes, materials and technologies. The study of thin films has greatly broadened the study of biomaterials by giving a clear indication of their chemical and physical properties. Knowledge of the mechanical, chemical, electrical and optical properties of any biomaterial thin films has to be established correctly in order to assign them to appropriate applications. Of late, significant development has been made in the study of thin films of biomaterials for various bioelectronics and biomedical applications. If

properly investigated and implemented, marine-derived biomaterials pose promising applications for mankind in various fields of optical, electronics and biomedical fields [1-11]. In particular, optical properties are directly related to structural and electronic properties of the materials, and hence very important in device applications. Such knowledge can provide a huge amount of information about their structure, optoelectronic behavior and transport of charge carriers [12, 13].

Chitosan is a polysaccharide derived from naturally occurring chitin which is largely found in marine invertebrates, insects, fungi and yeast [14]. Pure chitin is completely acetylated. However, when it is deacetylated, its derivative is known as chitosan. There is no set definition in the literature for the acetylation/deacetylation cut-off between chitin and chitosan but it is generally accepted that chitin must be at least 30–40% acetylated, though natural samples are typically 85–95% acetylated [15]. Studies have demonstrated that the different geographical sources and species of chitosan are able to alter the functional properties of resulting chitin and

chitosan [16, 17]. In Coastal Kenya and in particular Kilifi County, marine solid waste disposal is carried out negligently and without proper understanding of the nature of these materials. Therefore, the purpose of this study was to investigate the mechanical properties of chitosan from squid gladii found along the Kenyan Coast. This study was motivated by the fact that squid gladii are readily available as biomaterial waste material from the local fish industry along the Kenyan Coast. From the study, two relaxation processes; β -relaxation occurring between 293K and 323K and the α -relaxation hereby referred to as glass transition (T_g) occurring between 393K and 423K are revealed. Further, chitosan has been shown to be a viscoelastic (i.e. it both behaves as elastic (Hookean) solid and viscous (Newtonian) liquid with a very low mechanical damping which means its rigidity and resistance to deformation is very high. The study has hence helped to unveil the operating temperatures of the biomaterial.

2. Experimental

2.1. Sample Preparation

Samples of squid gladii (SG) were collected from the surrounding fish industries in the Kenyan coast. The collected SG samples were washed with water and then soaked in mild sodium. This was followed by washing and air drying at room temperature for two days. The dry SG were then pulverized into powder using a mortar and pestle and then sieved with a 1.5mm sieve to obtain squid gladii powder (SGP). Demineralization was done by putting the SGP in mild hydrochloric acid solution (1 M HCl) at a ratio of 1:10 w/v for 2 hours. This was followed by the filtering and washing with distilled water. The deproteinization step was done by putting the demineralized SGP in a mild sodium hydroxide solution of 5% w/v NaOH at 70° C at a ratio of 1:10 w/v overnight. The resulting chitin was filtered and washed with distilled water until neutral pH was reached. The samples were then dried in a hot air oven at 60° C for six hours and then weighed. The dry chitin powder obtained was refluxed in concentrated sodium hydroxide solution of 50% NaOH at 100°C for six hours in the ratio 1:10 w/v. The resulting chitosan was washed thoroughly with distilled water and dried in hot air oven at 60°C for 8 hours and then weighed. The dry chitosan powder was then stored in a desiccator.

Two different chitosan film samples were made. The first one (sample A) of 0.5% concentration was made by dissolving 0.5g of chitosan powder in a 100ml of 1% aqueous acetic acid solution with subsequent stirring to promote dissolution. The other (sample B) of 1% concentration was prepared by dissolving 1g of chitosan powder in a 100ml of 1% aqueous acetic acid. The obtained solutions of CAcOH were then filtered to remove insoluble residues. Plastic petri dishes were cleaned in soap water to eliminate any possible impurity and subsequently rinsed in distilled water. The cleaned petri dishes were then dried in hot air oven kept at 60°C. Free standing chitosan films were prepared by the solution casting method by pouring 10ml of the CAcOH solution into the cleaned petri

dishes on a flat bench and ensuring that the solution evenly covers the whole base. The solution was then allowed to evaporate naturally at room temperature for 72 hours. The resulting chitosan films were gently detached from the petri dishes, their thicknesses measured and then stored in a desiccator. Some other chitosan films were prepared by the drop casting method. In this method, two drops of the filtered chitosan-acetic acid solution were put on cleaned glass substrates. To ensure uniform thickness, the drops were smeared on the slides by rolling a glass rod once. The slides were then kept in a dust free area for drying at room temperature for 12 hours.

2.2. DMA Characterization

DMA equipment (TA instruments DMA 2980 was used to investigate the relaxation events and the viscoelastic response of the chitosan films. The instrument was first calibrated according to the manufacturers' recommended procedures. The measurements were conducted at a heating rate of 50 C/min, testing temperature ranging from 25-200°C, varied loading times and varied frequencies. The dimensions of the testing sample were; thickness 0.07 mm, width 9.44 mm and length 15.21 mm. The loss and storage moduli were recorded in a DMA multi-frequency single cantilever mode system. The storage and loss moduli were measured in the frequency range 0.1-15 Hz. The temperature range was from 298 to 373K in steps of 2K after every frequency sweep.

3. Results and Discussion

3.1. Effect of Temperature on Relaxation Time

To observe the effects of factors on relaxation processes, graphs of storage modulus and loss modulus against temperature at various frequencies (0.3Hz-15Hz) were plotted as shown in Figure 1. The storage modulus corresponds to the real component of the complex modulus ($E^* = E' + iE''$ where $i = -1^{1/2}$) and is the measure of the sample's stiffness while the loss modulus E'' corresponds to the imaginary component and is the measure of the damping capability of the sample. It was observed that storage modulus of the material increased at low temperatures and then decreased at higher temperature which is related to the increase in viscosity and polymer chain mobility of the matrix at higher temperatures.

It is understood that the loss factor ($\tan \delta$) is related to the ratio between the amount of mechanical energy lost and the stored energy during a cycle. The loss modulus is given by $\tan \delta = E''/E'$ and gives details of transitions taking place during heating processes ($\tan \delta$ peaks). Thus, in order to understand the transitions that took place on the chitosan thin films, the samples were heated between the temperature ranges of 303K and 473K. This was done for different frequencies. Figure 2 shows plots of loss factor ($\tan \delta$) versus temperature for frequency range between 3Hz and 20Hz.

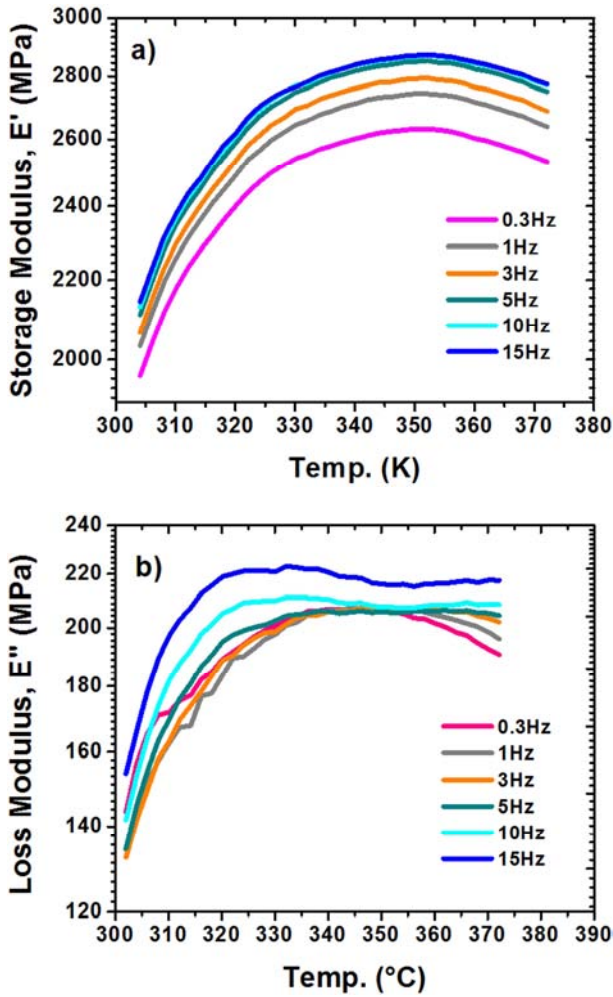


Figure 1. Graphs of storage modulus (a) and loss modulus (b) versus temperature showing the effects of frequency on the relaxation processes of chitosan thin film heated between 303K and 373K.

From the graph in Figure 2, two basic relaxation processes in the above mentioned range of temperatures and frequencies were observed. The two transitions (delta peaks) were noted in the temperature range of 303K – 323K and at 403K-423K. Both the peaks seemed to increase with frequency. The first delta peak is in agreement with the values of Mucha and coworkers who reported $\tan \delta$ peaks for chitosan thin films between 303K and 323K [18, 19]. On one hand, this transition occurring at low temperature can be assigned as the β -relaxation and attribute it to the local side-chain movement of the polymer (short range movement of polymer chains). In this temperature regime, the relaxation process can be caused mainly by the influence of water, the presence of which may lead to the emergence of hydrogen bonds with $-\text{OH}$ and $-\text{NH}_2$ groups or acetic acid, evaporating in this temperature region (plasticization effect). On the other hand, the second transition can be assigned to α -process (403K-423K) and is due to the glass transition (T_g) of the chitosan film. The broad $\tan \delta$ peaks show that the glass transition temperature occurs over a temperature range and not at a particular temperature. Important to note is that the value of T_g of chitosan depends on

many factors such as DDA, the water content, the source and the equipment. Examples of values of T_g reported are such as; Toffey and coworkers noticed α -relaxation between 333K and 367K for ionic complexes of chitosan [20]. In this study, this value of relaxation temperature increased for amidized chitosan derivatives. Ratto and coworkers reported glass transition temperature at 403K [21]. Sakurai reported T_g of chitosan at 476K. They however observed other transitions between 553K and 594K which were associated with a partial and total decomposition of the chitosan [22, 23].

Interestingly, the α -process (loss factor peaks) were observed to shift to higher temperature (increased T_g) with increasing frequency. The shift can be attributed to the fact that at low frequency, almost all the chains were able to follow the movement of the oscillations. However, at higher frequency, it became very difficult for all the chains to follow the movement of the oscillations. This can be explained by the fact that when the timescale of molecular motion coincides with that of mechanical deformation, each oscillation is converted into the maximum possible internal friction and non-elastic deformation occurs. The loss modulus, which is a measure of this dissipated energy, was observed to reach a maximum. There was also an increase in the loss factor near the glass transition that suggests the rapid increase in viscosity at temperatures close to the glass transition temperature. Furthermore, the peaks broadened with frequency suggesting broad distribution of T_g . This fact suggests that this is a true relaxation process. From these results, knowing the temperature at which the two transitions occur may give an insight of operating temperature range of the polymeric biomaterial.

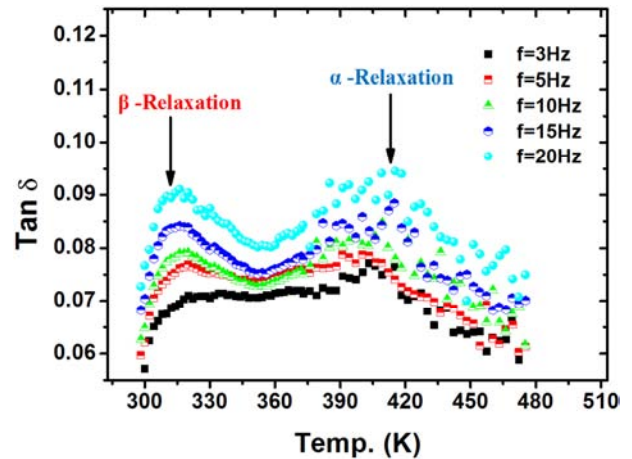


Figure 2. A graph of $\tan \delta$ (loss factor) as a function of temperature for oscillating frequency range of 3Hz and 20Hz showing $\tan \delta$ peaks for β and α -relaxation processes.

3.2. Frequency Dependence of Relaxation Time

From the frequency scans at different temperatures (298K-373K) on different samples, Figure 3 shows log plots of both the storage modulus (E') and the loss modulus (E'') as a function of frequency. As can be observed in Figure 3, there was a slow decrease in E' observed for low frequencies for all

the temperatures followed by rapid increase at high frequencies. Concurrently, a stronger increase in the loss modulus was observed above 5 Hz. From Figure 3 (a), the increase in the value of E' with frequency up to 15Hz may be attributed to the lesser mobility of polymeric chains at higher frequency. That is, as the frequency increased, it became

difficult for the polymer chains to respond to the applied forces and so they tended to remain in a frozen state. A frozen system stores more energy than a free system. However, E' became unstable and decreased after 15Hz. Figure 4 shows temperature dependence $\tan \delta$ plotted logarithmically against frequency for chitosan films.

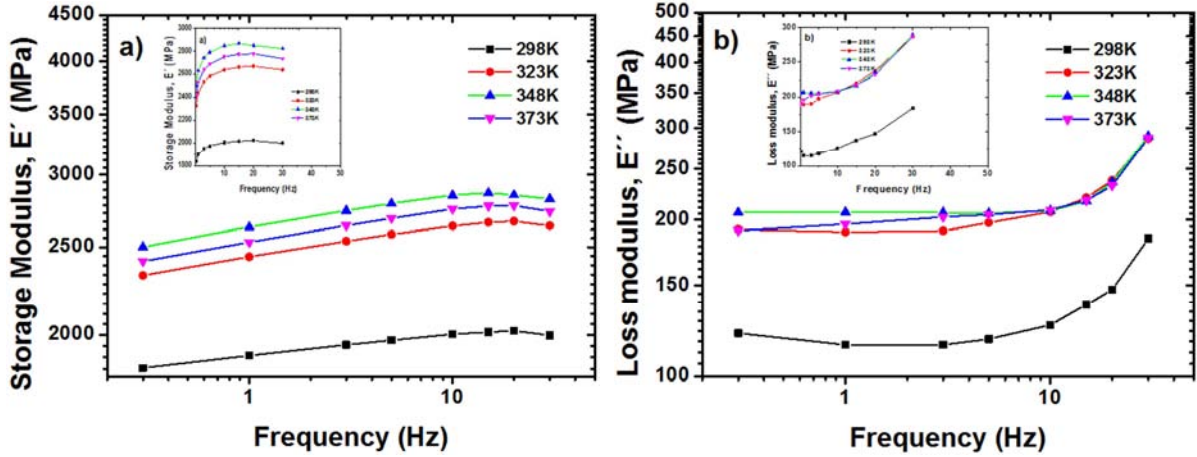


Figure 3. Log plots of storage modulus a) and loss modulus b) of chitosan films at different temperatures, measured as a function of sweep frequency. The linear plots are shown in the insets.

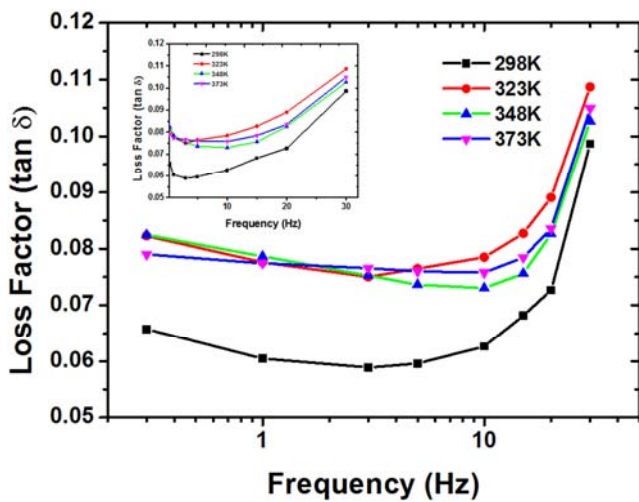


Figure 4. Loss factor of chitosan films at different temperatures, measured as a function of frequency. Linear plot is shown in the inset.

From the graph, there was a slow decrease in $\tan \delta$ observed for low frequencies for all the temperatures followed by a stronger increase above 3 Hz. The increase in $\tan \delta$ suggests rapid increase in viscosity at higher frequencies.

3.3. Time-Temperature Dependence of Relaxation Processes

Linear viscoelastic properties are both time-dependent and temperature-dependent. In order to understand the time-temperature dependence relaxation processes of the chitosan thin films, graphs of storage modulus and loss modulus versus time were plotted as shown in Figure 5 and Figure 6.

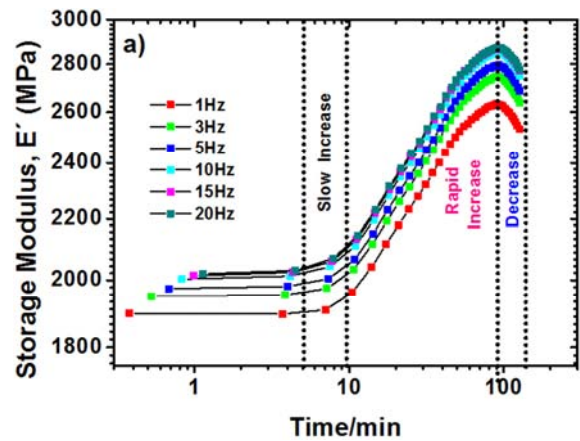


Figure 5. Storage modulus, E' of chitosan films at different frequencies, measured as a function of the loading time.

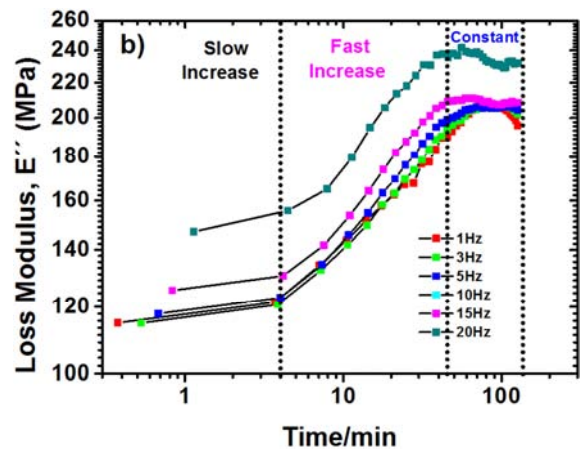


Figure 6. Loss modulus, E'' of chitosan films at different frequencies, measured as a function of the loading time.

From Figure 5, there was rapid increase of the storage modulus for the first 40 minutes followed by a slowed increase for the next 40 minutes before slow decrease. On the other hand, there was fast increase in loss modulus for the first 40 minutes followed by independence change with time as shown in Figure 6.

3.4. The Frequency Dependent Viscoelastic Properties

Further, the variation of the loss factor with the loading time was investigated. Figure 7 shows the dependence of loss factor with time as a function of frequency.

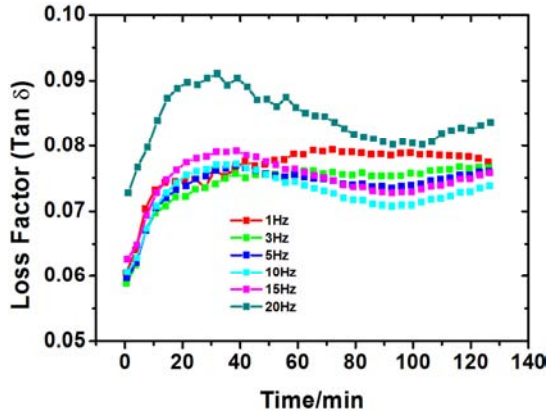


Figure 7. A graph of loss factor ($\tan \delta$) as a function of loading time for frequency range of 1Hz and 20Hz.

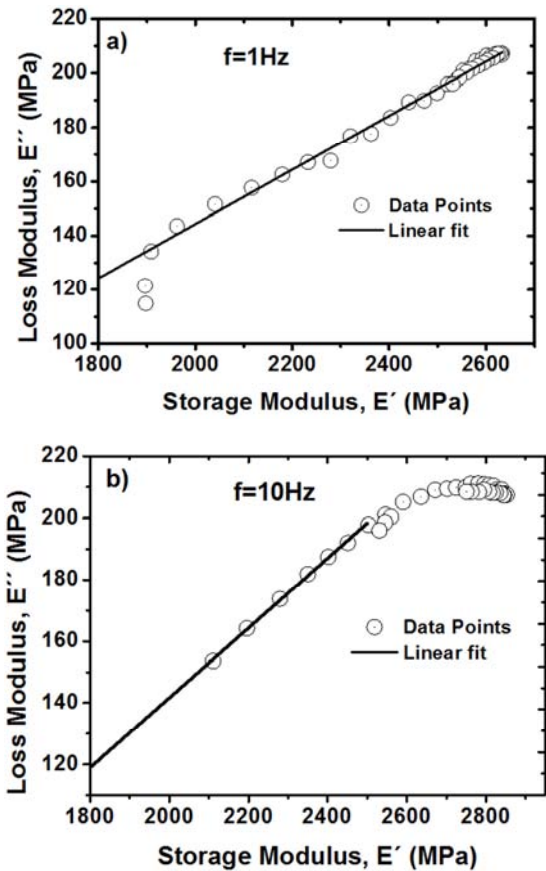


Figure 8. Loss modulus versus storage modulus for frequency $f=1\text{Hz}$ (a) and $f=10\text{Hz}$ (b).

From the graph in Figure 8, a linear relationship between E'' and E' giving a phase difference between $0 - 90^\circ\text{C}$ was observed. This indicates that chitosan is viscoelastic (i.e. it both behaves as elastic (Hookean) solid and viscous (Newtonian) liquid. From the graph of loss factor versus frequency as shown in Figure 9, it can be concluded that chitosan has very low mechanical damping which means its rigidity and resistance to deformation is very high. Thus, the viscoelastic characterization reported in this work for chitosan is useful in its use for a variety of biomedical applications.

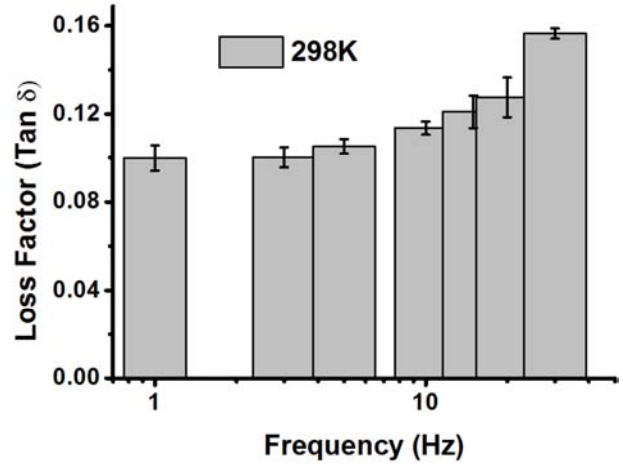


Figure 9. Loss factor versus frequency for temperature of 298K showing an increase.

4. Conclusion

This work presents the extraction and characterization of a biopolymer chitosan films found along the Kenyan coast. From the study, two relaxation processes; β - relaxation occurring between 293K and 323K and the α - relaxation hereby referred to as glass transition (T_g) occurring between 393K and 423K can be reported. These results show that chitosan is a potential biomaterial for biotechnological industries especially for the fabrication of bio-batteries and bio-sensor devices not only in terms of its structural, electrical and optical characteristics but also due to its product cost and environmental safety.

Acknowledgements

The authors would like to extend our sincere gratitude to Dr. Merenga of Kenyatta University for his productive discussions. Many thanks also goes to Pwani University for the financial support during the data collection phase.

References

[1] C. K. Pillai, W. Paul, and C. P. Sharma, *Prog. Polym. Science*, 34 (7): 641–678, 2009.
 [2] T. H. Silva, A. Alves, B. M. Ferreira, J. M. Oliveira, L. L. Reys, R. J. F. Ferreira, R. A. Sousa, S. S. Silva, J. F. Mano, and R. L. Reis, *International Material Reviews*, 57 (31): 276–306, 2012.

- [3] H Du, M. Liu, X. Yang, G. Zhai, *Drug Discovery Today*. 2015; 20 (8): 1004-1011.
- [4] M. Prabakaran, *International Journal of Biological Macromolecules*. 72: 1313-1322, 2015.
- [5] R. Y. Basha, S. Kumar, M. Doble, *Materials Science and Engineering: C*. 57: 452-463, 2015.
- [6] H. Du, M. Liu, X. Yang, G. Zhai, *Drug Discovery Today*, 20 (8): 1004-1011, 2015.
- [7] M. Prabakaran *International Journal of Biological Macromolecules*, 72: 1313-1322, 2014.
- [8] R. Y. Basha, S. Kumar, M. Doble, *Materials Science and Engineering, C*. 57: 452-463, 2015.
- [9] M. Malerba and R. Cerana, *Polymers*, 10:(2), 118-124, 2018.
- [10] A. Baranwa, A. Kumar, A. Priyadarshini, GS. Oggu, I. Bhatnagar, A. Srivastava, P. Chandra, *Int J Biol Macromol*. 110: 110-123, 2018.
- [11] A. K. Y. Salman, Gh O. Abdullah, R. R. Hanna, B. A. Shujahadeen, *Int. J. Electrochem. Sci.*, 13: 3185-3199, 2018.
- [12] R. K. Singh, Y. W. Zhang, N. P. Thao, N. M. Jeya, and J. K. Lee, *Applied microbiology and macromolecules*, 89 (2): 337-344, 2010.
- [13] M. A Meyers, Chen Po-Yu, A. Y. Lin and Y. Seki, *Progress in Materials Science*, 53: 1 to 206, 2008.
- [14] I. G. Austin, A. J. Springthorpe, B. A. Smith and C. E. Turner, *Proceedings of the Physical Society*, 90 (1), 1981.
- [15] R. A. A. Muzzarelli. *Chitin nanostructures in living organisms*, volume 34. Springer, Netherlands, 2011.
- [16] A. Domard, *Carbohydrate Polymers*, 84 (2): 696-703, 2012.
- [17] M. Rinaudo, *Progress in Polymer Science*, 31 (7): 603-632, 2006.
- [18] M. Mucha and A. Pawlak, 427 (1 - 2): 69-76, 2005.
- [19] S. Rivero, M. A. García and A. Pinotti, *Adv. Mat. Lett.*, 4, 10, 578-586, 2014.
- [20] A. Toffey and W. G. Glasser. Chitin derivatives iii formation of amidized homologs of chitosan. 8 (1): 35-47, 2001.
- [21] J. Ratto and T. Hatakeyama. DSC investigation of phase transition in water/chitosan system. 36: 2915-19, 1995.
- [22] K. Sakurai, T. Maegawa, and T. Takashi, *Polymer*; 41: 7051-7056, 2000.
- [23] K. Sakurai, H. Tanaka, N. Ogawa, T. J. Takahashi, *Macromol Sci Phys B*, 36: 703, 1997.